Role of the Bilayer−Bilayer Interaction on the Ripple Structure of Supported Bilayers in Solution

ARTICLE *in* THE JOURNAL OF PHYSICAL CHEMISTRY · SEPTEMBER 1996

Impact Factor: 2.78 · DOI: 10.1021/jp961054r

Role of the Bilayer−Bilayer Interaction on the Ripple Structure of Supported Bilayers in Solution

Ye Fang and Jie Yang*

Physics Department, University of Vermont, Cook Building, Burlington, Vermont 05405

Received: April 8, 1996; In Final Form: June 6, 1996[⊗]

We have developed a method to prepare supported double bilayers made of phospholipids to facilitate in-solution studies of the bilayer−bilayer interaction of biologically relevant model membranes. It is found that a ripple structure, with an average wavelength of 27 nm, appears at room temperature in the double-bilayer region only. Some large ripples, of an average wavelength of 53 nm, are also observed on the double-bilayer region and are extremely soft and flexible. These experimental observations demonstrate that the bilayer−bilayer interaction may play a role to induce the formation of the ripple structure in our system. We also found that the formation of the ripple structure takes a few minutes or less while cooling to room temperature, and the relaxation of the ripple structure takes over 10 h at room temperature or 4 °C.

Introduction

The ripple phase in phosphatidylcholine (PC) bilayers, first discovered by Tardieu et al.,[1] has a distinct structural characteristic, in which the lipid bilayer has a regular spatial modulation.[2,3] Electron microscopy and X-ray diffraction on multilamellar PC bilayers show that typical wavelengths of bilayer ripples are 12−16 nm or double those values.[1,4−7] Macroripples, presumably due to some topological defects, are also present in multilamellar vesicular bilayers.[7−9] The ripple wavelength in multilamellar vesicles varies slightly as the water content or the temperature changes[10−12] and also increases slightly with the incorporation of cholesterol.[13,14] The ripple structure also persists at temperatures below the pretransition temperature in lipid mixtures containing glycolipids.[15] Recently, atomic force microscopy (AFM) at room temperature showed that tris(hydroxymethyl)aminomethane (Tris), a chemical compound, induces the ripple structure in supported unilamellar PC bilayers in solution.[16] Ion-induced ripples in supported asymmetric unilamellar bilayers have also been observed.[17] These results indicate that the ripple structure forms under various conditions.

Several theoretical models have been proposed to understand the mechanism of the ripple formation. Assuming a membrane made of straight chains, with the angle between the local surface tangent and the straight chain as the order parameter, Doniach showed that a ripple structure can exist in the model bilayer.[18] Considering a simplified 1-D model composed of connected "molecules" with a head and a straight tail, Carlson and Sethna showed that a stable ripple phase exists as a result of ordering of topological defects.[19] Constructing a 2-D phenomenological Landau Hamiltonian to account for couplings between membrane curvature and molecular tilt, Lubensky and Mackintosh demonstrated that a ripple structure exists in a narrow temperature range at the reduction of the membrane longitudinal elastic constant.[20] These models suggest that the ripple structure may exist in a unilamellar bilayer as a result of some lipid−lipid interactions in the bilayer. However, bilayer−bilayer interactions have been also conjectured to play a role in the ripple formation.[21] Because of the complicated nature of a lipid bilayer, these theoretical modeling studies may not account for all factors in experiments on different bilayers under various conditions.

We have developed a method to prepare supported double bilayers on mica by the fusion of vesicles. This method facilitates the comparison of structural features on top of the double bilayer with those on top of the unilamellar bilayer, and the results of which may provide information about the bilayer−bilayer interaction. The use of low-salt solution (20 mM NaCl) minimizes any effect due to ions on the ripple formation in our experiments. The capability of operating AFM in solution[22−25] allows us to study the structure of supported bilayers with in situ AFM. For supported dipalmitoylphosphatidylcholine (DPPC) bilayers, we detected the existence of a ripple structure in double-bilayer regions only, indicating that the bilayer−bilayer interaction may play a role in the formation of the ripple structure in our systems. A majority of the ripple structure has an average wavelength of 27 nm and an average amplitude of 0.5 nm (we call it the "normal" ripple structure). Some large ripples, often coexisting with the "normal" ripples, have an average wavelength of 53 nm and largely fluctuated amplitudes of an average of 8 nm. The amplitude and the fluctuation of the large ripples decrease as the probe force increases, and the amplitude of the "normal" ripples does not change for probe forces as large as 3 nN. We also observed an extremely slow relaxation of the ripple structure. The ripple structure can be induced repeatedly, but the pattern of formed ripples varies under different initial conditions. Although double bilayers with a high surface coverage are reliably formed, our method does not result in the formation of supported triple or multilamellar bilayers.

Experimental Section

DPPC lipids in the powder form were obtained from Sigma (St. Louis, MO) and used without further purification. Small unilamellar vesicles were prepared by sonicating a fresh lipid suspension until clear[26,27] by using a Fisher FS3 ultrasonic cleaner. The suspension, about 0.5 mg/mL of lipids in 20 mM NaCl, was in a culture tube under nitrogen gas. The unilamellar vesicles were then purified by centrifuging at 14 000 rpm for about 30 min. Specimens of supported unilamellar bilayers were prepared by the vesicle-fusion method as previously reported.[16,28] A supported unilamellar bilayer was transferred to a homemade fluid cell for AFM imaging. During specimen transfer, care was taken to avoid any exposure of the supported bilayer to air.

[⊗] Abstract published in *Advance ACS Abstracts,* September 1, 1996.

S0022-3654(96)01054-4 CCC: $12.00

Supported unilamellar bilayers, with over 95% surface coverage, were used to prepare supported double bilayers. The unilamellar bilayer was covered by a droplet (about 150 μL) of 20 mM NaCl. Then, a small volume of lipid suspension (150 μL at 0.5 mg/mL) was added to the droplet. Afterward, the sample was kept at a temperature of 4 °C for over 48 h and then heated to 50 °C for about 60 min. To wash out excess vesicles in the droplet, about 20 exchanges with 200 μL of 20 mM NaCl were made. This method usually produces a double bilayer with the upper bilayer at a surface coverage over 70%. Although the method described above allows us to prepare reliably supported double bilayers, we are not able to prepare reliably supported triple or multilamellar bilayers. This failure indicates that the underlying mechanism of the formation of supported bilayers might be complicated.

A NanoScope E AFM and oxide-sharpened Si_3N_4 tips with a nominal spring constant of 0.06 N/m, all from Digital Instruments (Santa Barbara, CA), were used in this work. Most images were obtained under a probe force of about 0.5 nN, at a pixel number of 512 × 512, and with a scanning line speed of about 5 Hz. For the study of elastic properties of the ripple structure, the probe force is changed between about 0.5 nN and about 3 nN.

Results

Although underlying mechanisms are not clear, direct fusion of vesicles onto a flat hydrophilic surface has been a reliable method to prepare stable supported unilamellar bilayers.[16,28] On this basis, we expect the formation of a second bilayer on top of the supported unilamellar bilayer, since the supported bilayer is flat and lipid headgroups are hydrophilic. Using a modified vesicle-fusion method, we produce stable supported double bilayers of DPPC with a mean coverage of over 70%. Figure 1 shows several typical images of supported DPPC membranes. Supported unilamellar membranes are always planar with some defects (Figure 1, part a). Large membrane defects, naturally existing or created by an AFM tip, can be used to determine the bilayer thickness at their edges. The thickness of supported unilamellar DPPC bilayers in our experiments is about 6 nm, consistent with other studies.[16,29] Figure 1, parts b and c, show two typical examples of supported double-bilayer membranes. In both images, bilayer ripples exist in the upper bilayer, and defects in the lower bilayer reveal convincingly the double-bilayer structure. The thickness of the rippled upper bilayer is about 7 nm.

The ripple structure has several unique patterns. Smooth bending of ripples is a dominant feature. However, some turns have a 120° bending (Figure 2, part a), and several ripples have an overall bending angle of about 60° in which the turning region is rather smooth (Figure 2, part b). We observed extended ripples which are commonly observed with electron microscopy and some short ripples (Figure 2, part d). The wavelength of these ripples averages about 27 nm, with an average amplitude of about 0.5 nm. We note that these ripples are similar to those so-called 2λ-ripples.[3] Yet, we did not observe the characteristic double-edged structure[3,16] nor did we observe any λ-ripple structure.[3]

Our AFM images show that often a group of ripples ends by meeting another group of ripples oriented at a different angle (see Figure 2, part c). This phenomenon indicates that there may exist several nucleation centers around which the ripples grow at different orientations. In this scenario, we can imagine that the ripple grows along the ridge, and the ripple may be hindered as it meets another rippling ridge at a different orientation and thus stops the growing.

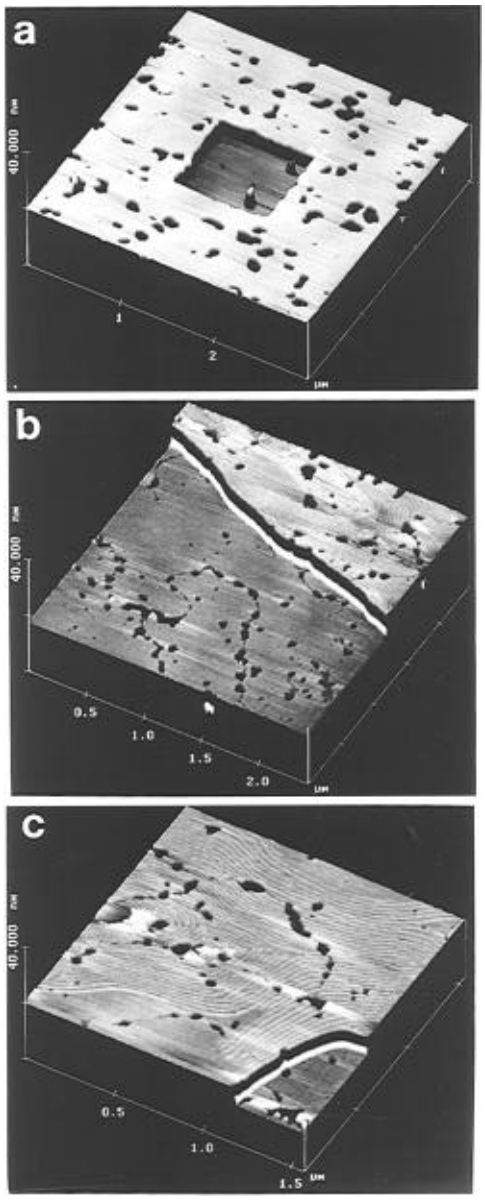

Figure 1. AFM images of mica-supported bilayers of DPPC in 20 mM NaCl at room temperature (about 23 °C). Supported unilamellar bilayer of DPPC in part a has a thickness of about 6 nm and is planar with some defects. A square defect at the center is created by AFM tip at a probe force of about 10 nN, a scanning line speed of 244 Hz, and a scanning window of 1 μm^2. Two typical AFM images of supported double bilayers of DPPC prepared by a modified vesicle-fusion method are shown in parts b and c. Bilayer ripples on the upper bilayer in both cases are seen here, and defects in the lower bilayer confirm the double-bilayer structure.

Another interesting feature, as shown in Figure 2, parts a and b, is the spatial arrangement of some bilayer defects on the ripples. It can be seen that some defects in these images cut through continuous ripples. This phenomenon indicates that the ripple structure must have been formed before the occurrence of these bilayer defects. Further, the size and the shape of these defects also rule out the possibility that they are gaps created by some mechanical strains. Some loss of lipid molecules must accompany the creation of these defects, although details of the process are unclear.

Figure 2, parts e and f, are sectional plots, corresponding to the lines in Figure 2, parts c and d, respectively. From these original sectional plots, we see that the signal to noise ratio is not high enough for statistical averaging to analyze the detailed

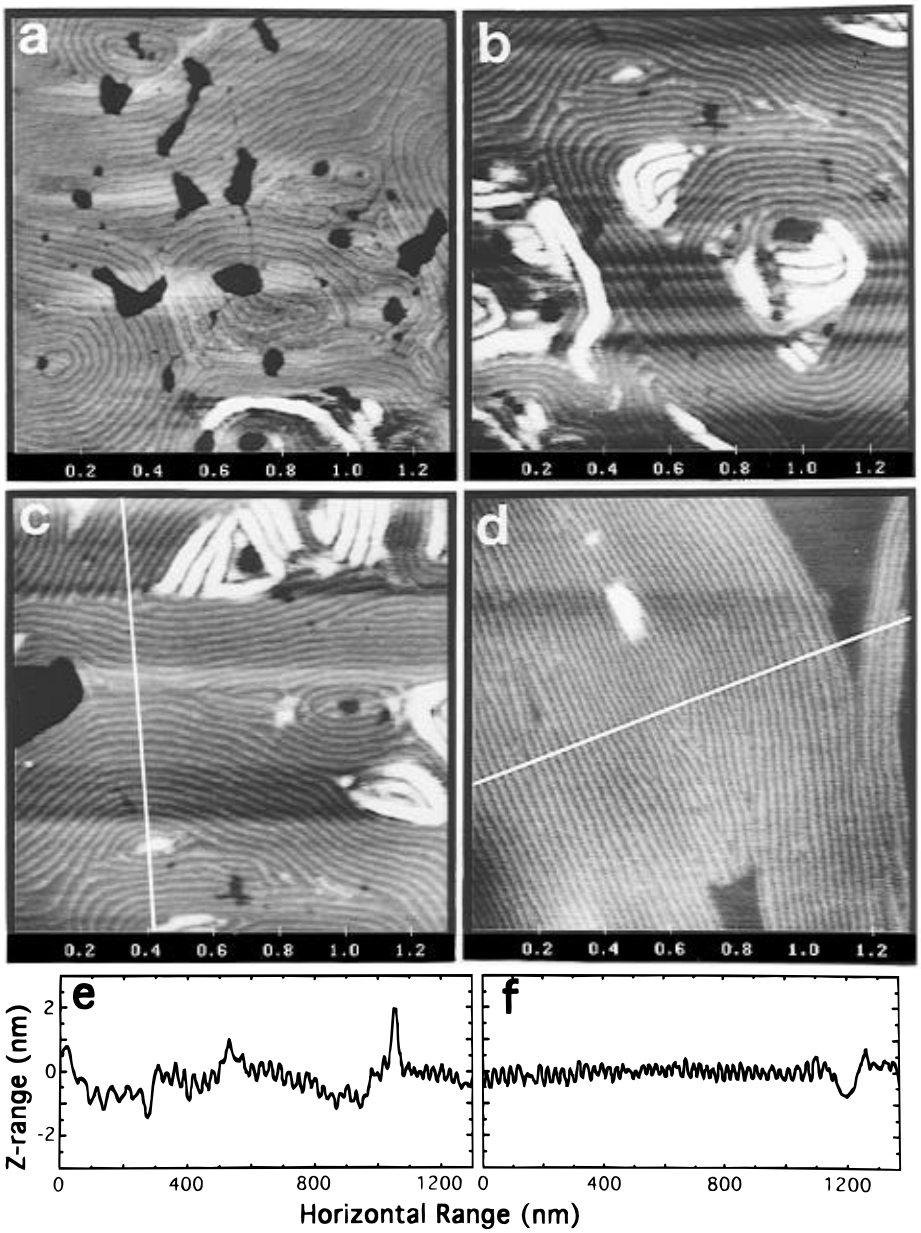

Figure 2. Four typical AFM images of the ripple structure in upper bilayers. In a, many defects cut through ripples. In parts a−c, there are some of the large ripples. Some ripples with a bending angle of 120° are seen in part a, and several ripples with an overall bending angle of 60° yet a smooth curving at the turn are seen in part b. Ripple boundaries by meeting ripples of different orientations are seen in part c. In part d, we see long and extended ripples, with some areas being planar. Graph unit: μm. Section plots, corresponding to the lines in parts c and d, are shown in parts e and f.

spatial shape of the ripple structure beyond an average amplitude. The ripple amplitude as measured from AFM images is an underestimation, because of the finite radius of the tip that prevents the tip from reaching the ripple node. Thus, the average amplitude of the ripple structure is much smaller than the thickness at the edge of the ripple structure, as can be seen in Figure 2, part f. Figure 3 contains four Fourier transforms, corresponding to Figure 2, parts a−d, respectively. The main feature of the ripple structure from these Fourier transforms is the lack of a perfect, long-range, spatial order. This feature may reflect a characteristic of our system: the ripple structure is not a true thermal equilibrium state of the bilayer at room temperature.

We also observed the large ripples, which either coexisted with the "normal" ripples (see Figure 2, parts a and c) or solely existed (see Figure 4). The large ripples have similar structures as those macroripples observed elsewhere.[7,8] Taking the advantage of in situ AFM, we studied mechanical strength of the "normal" and the large ripples. For the "normal" ripples, both the wavelength and the amplitude remain unchanged for probe forces as large as 3 nN. For the large ripples, however, the amplitude is strongly and reversibly dependent on the probe force applied. Figure 4 shows an example. At a probe force of about 0.6 nN, the large ripples in Figure 4, part a, have a wide distribution in their large amplitude, 8 ± 6 nm for 57 measurements. When the probe force increases to about 2 nN, their amplitudes decrease and have much less fluctuation, 4 ± 1 nm for 70 measurements (Figure 4, part b). However, the wavelength of the large ripples remains unchanged with the increase of the probe force (53 ± 7 nm).

Although there are regions, on the upper bilayer, with full coverage of the ripple structure within several square microns, we also observed a few of upper bilayer regions with a planar structure. An example is shown in Figure 5. Here we see many short ripples, indicating again that the observed ripple structure may not correspond to the true stable structure in thermal

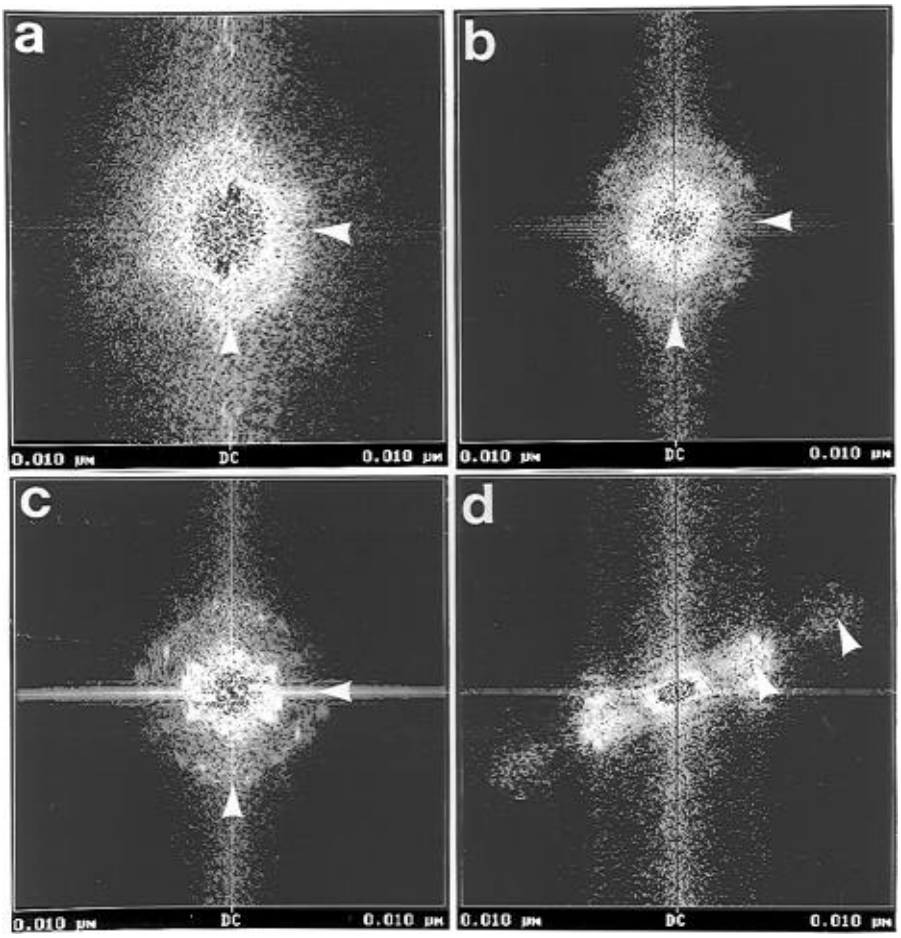

Figure 3. Fourier transforms corresponding to Figure 2, parts a−d, are shown in parts a−d, respectively. Arrows indicate the Fourier space points corresponding to the reciprocals of the real space distances: part a, 27 nm (horizontal arrow) and 25 nm (vertical arrow); part b, 26 nm (horizontal arrow) and 25 nm (vertical arrow); part c, 25 nm (horizontal arrow) and 25 nm (vertical arrow); part d, 26 nm and 13 nm (tilted arrows).

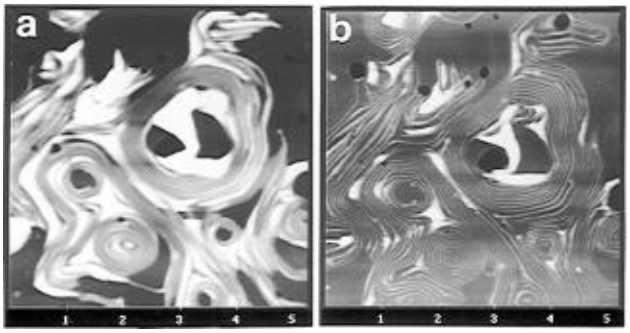

Figure 4. Pair of images of the large ripple structure under different forces. In parts a and b, the probe forces were about 0.6 and 2 nN, respectively. The amplitude of the large ripples changes appreciably. The change is reversible as the probe force varies. Graph unit: μm.

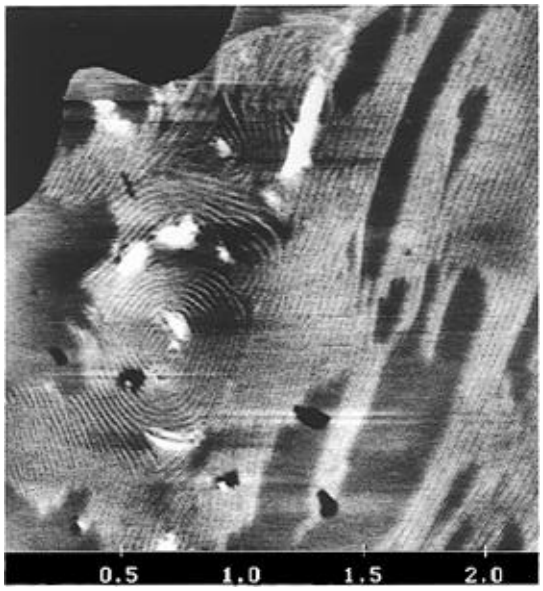

Figure 5. Typical image to demonstrate the relaxation of ripples. We see here that many regions of the upper bilayer are planar without any ripples. Many ripples are rather short. We also observe defects cutting through ripples. The upper left corner is the lower bilayer. Due to the limited image depth, the lower bilayer appears totally dark. Graph unit: μm.

equilibrium at room temperature. During the AFM imaging, which usually took several hours, we did not observe any degradation of the ripple structure. However, after keeping the samples at room temperature or 4 °C overnight, we observed the fade of the ripples, accompanying by the appearance of more short ripples and many flat bilayer regions. The thickness of the flat upper bilayer is about 6 nm, consistent with that of the unilamellar planar bilayer. We also found that by heating the flat double-bilayer specimen for several hours at 40, 50, or 60 °C, the ripple structure reappears after the specimen was cooled to room temperature under ambient conditions. The pattern of the reappeared ripple, however, is somewhat different from that of the original ripples. Therefore, the ripple structure on the double bilayer has a finite, although very long, relaxation time at room temperature.

Discussion

Membrane−membrane interactions, which might be mediated by proteins *in vivo*, play a crucial role in many biochemical processes.[30] In lipid bilayers, the bilayer−bilayer interaction acts through bound water molecules which are ordered with a large steric energy.[31] In fatty acid films, atomic resolution imaging showed packing differences between layers which were believed to be a result of the headgroup interaction between the layers.[32−34] Our supported double bilayers offer additional systems to study the bilayer−bilayer interaction experimentally. The large PC headgroup usually is bound with over 10 water molecules, and there are hydration layers between the PC bilayer and the substrate and between adjacent PC bilayers.[31,35,36] Since the coupling between monolayers in a bilayer is much stronger than that between bilayers and between the bilayer and the substrate,[36] we assume that the bilayer is one entity in our system. In this system, the bilayer−bilayer interaction should exist for the bilayers in the double-bilayer region, whereas the bilayer−substrate interaction should be the same for both the unilamellar and the double-bilayer regions. With in situ AFM, we can investigate structural features originated from the bilayer−bilayer interaction. The experimental results demonstrate clearly that the ripple structure appears only in the upper bilayer in the double-bilayer system. Thus the bilayer−bilayer interaction might be responsible for the formation of the ripple structure that occurred only in the double-bilayer regions. However, AFM imaging does not allow us to determine whether the ripple structure persists to the lower bilayer beneath the upper bilayer. Similarly, details of the bilayer−bilayer interaction cannot be revealed by the structural study alone.

Since the ripple structure is sensitive to various factors, such as the lipid species and ionic species,[4−17] we cannot draw the conclusion that the bilayer−bilayer interaction is the only source that induces the ripple structure. This is not in conflict with other studies where no ripple structure was observed on multiple bilayer systems.[37,38] Under different ionic conditions, the ripple structure in supported unilamellar bilayer has been detected, indicating that the bilayer−substrate interaction does not restrain the bilayer from the ripple formation.[16,17] In our systems, lipid bilayers are under a low-salt environment. Thus, ions in the solution should induce very little bilayer structural change. We also conducted control experiments with specimens containing supported unilamellar bilayers only, without observing any ripple structure, even though these specimens were treated exactly the same way as treating those double-bilayer specimens. Combining the results from the present study and those reported elsewhere,[16,17] we see that the ripple formation may involve a very delicate interplay between various factors, and a slight imbalance may be sufficient to induce the ripple structure. The simplicity of our system, that the bilayer is in the low ionic strength environment, favors the interpretation that in this system the bilayer−bilayer interaction may play a role to induce the ripple structure in the double-bilayer regions.

The later fading away of the ripple structure after being allowed to stand for a long time indicates that the ripple structure in our system may not be in the stable thermal equilibrium state at room temperature. This phenomenon is also reflected in our results that the average ripple wavelength is about twice the normal ripple structure (the so-called λ-ripple).[3] The so-called λ-ripple is known to have a long-range order, as demonstrated by the X-ray diffractional study and the study of the replica of rapidly frozen specimens.[4−15,39,40] The lack of the long-range order in our system is also demonstrated in the Fourier transforms, in which no strong diffraction spots, indicatives of a long-range order, are detected. The sectional plots also indicate that the fluctuation in the ripple amplitudes in our system is quite large, and thus we may not obtain any structural detail of the ripple shape with sufficient statistical significance other than an average amplitude.

A theoretical modeling study indicated that the lipid bilayer may have very weak mechanical strength, because of extremely low strain energy in the bilayer.[41] We here demonstrate experimentally that the large ripples are extremely soft, since their amplitudes decrease with a slight increase of the probe force. Furthermore, the large ripples are also extremely flexible, evidenced by the reversibility of their structure as the probe force varies. The amplitude of the "normal" ripples, on the other hand, is insensitive to the probe force and thus is mechanically much "stronger". However, "stronger" is meant in a relative sense since the largest probe force applied is about 3 nN only. These results suggest that mechanical properties of the ripple structure are very complicated. On the basis that the population of the large ripples is much less than that of the "normal" ripples, we may conclude that the "normal" ripple structure is more stable than the large ripple structure.

We further speculate if any energetics can be inferred from our results. For the large ripples, a probe force change from 0.6 to 2 nN causes the average amplitude to change from 8 to 4 nm. Thus the average work applied by the tip is about 6×10^{-18} J. Assuming a tip contact radius of 10 nm, we find there are about 10^{-21} mol of lipids in contact with the tip, if the surface area for each headgroup is taken to be about 50 Å^2.[35] Thus, on average, a strain energy of about 6 kJ/mol is stored in regions of the compressed large ripples at a probe force of about 2 nN, which is about 2.5 times the thermal energy at room temperature. The energetics for the "normal" ripples cannot be analyzed, because no obvious change in the ripple amplitude has been detected as the probe force increases to 3 nN. The response of the ripple structure to the probe force also suggests the unlikeliness that the ripple structure may be induced by some kind of tip−sample coupling, on the basis that the ripple wavelengths and the "normal" ripple amplitude are independent of the probe force applied and that the large ripple amplitude varies reversibly as the probe force changes. On the other hand, tip-induced structure is likely to change the spatial feature as the probe force changes, as shown in the tip-induced polymerization of polystyrene[42] in which the probe forces were much larger.

It may help us to understand the nature of our results by examining how the ripple structure is induced and by comparing our situation with other situations in other experiments on different systems. The formation of a double bilayer in our experiments requires a cooling procedure, in which the bilayer is heated to a high temperature (50 °C) and is followed by cooling to room temperature in ambient condition. For multilamellar vesicular DPPC bilayers in solution, the ripple phase exists between 35 and 42 °C.[1,4−7] Therefore, the ripple structure in thermal equilibrium may not be expected in DPPC bilayers at room temperature. In our system, it is possible that the ripple structure is induced above room temperature. The actual time required to induce the ripple structure can be estimated from our experiments on the reappearing of the ripple structure. In these experiments, the quality of the ripple structure remains the same whether the cooling starts from 60, 50, or 40 °C. The cooling to room temperature in ambient condition takes about 40 min or less, suggesting that the time taken to form the ripple structure may be minutes or less. This short time is in sharp contrast to the long time (tens of hours or more) required for the relaxation of the ripple structure. At present, it is not entirely

clear how this asymmetric behavior in the ripple formation and relaxation relates to the molecular details of the bilayer−bilayer interaction.

In conclusion, we have developed a method to prepare supported DPPC double bilayers with surface coverages over 70% in low-salt solution. Some ripple structures are observed in the double-bilayer regions only, suggesting that the bilayer−bilayer interaction may be responsible for inducing the ripple structure. Since the bilayer−bilayer interaction is mediated by lipid headgroups, our results also suggest that lipid headgroups play a role in inducing the ripple structure, consistent with other studies of supported unilamellar bilayers.[16,17] The ripple structure in our system has a rather asymmetric behavior in its formation and relaxation, which may be unique in supported bilayers.

Acknowledgment. We thank the two anonymous reviewers for their helpful comments and insights. Support from the U.S. Army Research Office and a American Heart Association Vermont Affiliated Grant in Aid is acknowledged.

References and Notes

(1) Tardieu, A.; Luzzati, V.; Reman, F. C. *J. Mol. Biol.* **1973**, *73*, 711.
(2) Parsegian, V. A. *Biophys. J.* **1983**, *44*, 413.
(3) Sackmann, E. In *Biophysics*; Hoppe, W., Lohman, W., Maarkl, H., Zieglar, H., Eds.; Springer-Verlag: Berlin, 1983; pp 425−430.
(4) Luna, E. J.; McConnell, H. M. *Biochim. Biophys. Acta* **1977**, *466*, 381.
(5) Ruppel, D.; Sackmann, E. *J. Phys. (Paris)* **1983**, *44*, 1025.
(6) Stamatoff, J.; Feuer, B.; Guggenheim, H. J.; Tellez, G.; Yamane, T. *Biophys. J.* **1982**, *38*, 217.
(7) Zasadzinski, J. A. N.; Schneider, M. B. *J. Phys. (Paris)* **1987**, *48*, 2001.
(8) Zasadzinski, J. A. N. *Biochim. Biophys. Acta* **1988**, *946*, 235.
(9) Brown, R. E.; Anderson, W. H.; Kulkavni, V. S. *Biophys. J.* **1995**, *68*, 1396.
(10) Janiak, M. J.; Small, D. M.; Shipley, G. C. *Biochemistry* **1976**, *15*, 4575.
(11) Matuoka, S.; Kato, S.; Hatta, I. *Biophys. J.* **1994**, *67*, 728.
(12) Wack, D. C.; Webb, W. W. *Phys. Rev. Lett.* **1988**, *61*, 1210.
(13) Copeland, B. R.; McConnell, H. M. *Biochim. Biophys. Acta* **1980**, *599*, 95.
(14) Scott, H. L.; McCullough, W. S. *Biophys. J.* **1993**, *64*, 1398.
(15) Rock, P.; Thompson, T. E.; Tillack, T. W. *Biochim. Biophys. Acta* **1989**, *979*, 347.
(16) Mou, J.; Yang, J.; Shao, Z. *Biochemistry* **1994**, *33*, 4439.
(17) Czajkowsky, D. M.; Huang, C.; Shao, Z. *Biochemistry* **1995**, *34*, 12501.
(18) Doniach, S. *J. Chem. Phys.* **1979**, *70*, 4587.
(19) Carlson, J. M.; Sethna, J. P. *Phys. Rev. A* **1987**, *36*, 3359.
(20) Lubensky, T. C.; Mackintosh, F. C. *Phys. Rev. Lett.* **1993**, *71*, 1565.
(21) Cevc, G.; Zeks, B.; Podgornik, R. *Chem. Phys. Lett.* **1981**, *84*, 209.
(22) Drake, B.; Prater, C. B.; Weisenhorn, A. L.; Gould, S. A. C.; Albrecht, T. R.; Quate, C. F.; Cannell, D. S.; Hansma, H. G.; Hansma, P. K. *Science* **1989**, *243*, 1586.
(23) Hui, S. W.; Viswanathan, R.; Zasadzinski, J. A.; Israelachvili, J. N. *Biophys. J.* **1995**, *68*, 171.
(24) Shao, Z.; Yang, J.; Somlyo, A. P. *Annu. Rev. Cell. Biol.* **1995**, *11*, 241.
(25) Yang, J.; Shao, Z. *Micron* **1995**, *26*, 35.
(26) Boni, L. T.; Minchey, S. R.; Perkins, W. R.; Ahl, P. L.; Slater, J. L.; Tate, M. W.; Gruner, S. M.; Janoff, A. S. *Biochim. Biophys. Acta* **1993**, *1146*, 247.
(27) Kantor, H. L.; Mabrey, S.; Prestegard, J. H.; Sturtevant, J. M. *Biochim. Biophys. Acta* **1977**, *466*, 402.
(28) Brain, A. A.; McConnell, H. M. *Proc. Natl. Acad. Sci. U.S.A.* **1984**, *81*, 6159.
(29) Tamm, L. K.; McConnell, H. M. *Biophys. J.* **1985**, *47*, 105.
(30) van Venetie, R.; Verkleij, A. J. *Biochim. Biophys. Acta* **1982**, *692*, 397.
(31) McIntosh, T. J.; Simon, S. A. *Annu. Rev. Biophys. Biomol. Struct.* **1994**, *23*, 27.
(32) Schwartz, D. K.; Garnaes, J.; Viswanathan, R.; Zasadzinski, J. A. N. *Science* **1992**, *257*, 508.
(33) Viswanathan, R.; Zasadzinski, J. A.; Schwartz, D. K. *Science* **1993**, *261*, 449.
(34) Viswanathan, R.; Madsen, L. L.; Zasadzinski, J. A.; Schwartz, D. K. *Science* **1995**, *269*, 51.
(35) Tristram-Nagle, S.; Zhang, R.; Suter, R. M.; Worthington, C. R.; Sun, W.-J.; Nagle, J. F. *Biophys. J.* **1993**, *64*, 1097.
(36) Merkel, R.; Sackmann, E.; Evans, E. *J. Phys. (Paris)* **1989**, *50*, 1535.
(37) Singh, S.; Keller, D. J. *Biophys. J.* **1991**, *60*, 1401.
(38) Brandow, S. L.; Turner, D. C.; Ratna, B. R.; Gaber, B. P. *Biophys. J.* **1993**, *64*, 898.
(39) Woodward, J. T., IV; Zasadzinski, J. A. *Phys. Rev. E.* **1996**, *E53*, R3044.
(40) Sun, W.; Tristram-Nagle, S.; Suter, R. M.; Nagle, J. F. *Bull. Am. Phys. Soc.* **1996**, *41*, 126.
(41) Sackmann, E. *FEBS Lett.* **1994**, *346*, 3.
(42) Leung, O. M; Goh, M. C. *Science* **1992**, *255*, 64.

JP961054R